ELSEVIER

International Journal of Mass Spectrometry 207 (2001) 167–182

International Journal of Mass Spectrometry

Measurements of benzene and toluene in ambient air using proton-transfer-reaction mass spectrometry: calibration, humidity dependence, and field intercomparison

C. Warneke[a,*], C. van der Veen[a], S. Luxembourg[a], J.A. de Gouw[a], A. Kok[b]

[a]*Institute for Marine and Atmospheric Research (IMAU) Princetonplein 5, 3584 CC Utrecht, The Netherlands Debye Institute,*
[b]*Department of Atomic and Interface Physics, Princetonplein 5, 3584 CC Utrecht, The Netherlands*

Received 9 November 2000; accepted 23 December 2000

Abstract

PTR-MS (proton transfer reaction–mass spectrometry) is a chemical ionization mass spectrometry technique that uses proton transfer reactions with H_3O^+ ions for on-line measurements of organic trace gases in air. The instrument is calibrated for benzene and toluene, and the humidity dependence is investigated. The observed humidity dependence is explained using a simple model that calculates the distribution of $H_3O^+ \cdot (H_2O)_n$ ($n = 0, 1, 2, 3$) cluster ions in the reactor. These findings were verified in a field intercomparison by comparing PTR-MS measurements of benzene and toluene with GC (gas chromatograph) analyses of gas samples. Isoprene, acetone, acetonitrile, methanol, dimethyl sulfide, and acetaldehyde were also investigated, and no humidity dependence was found, except for isoprene, when larger clusters were used as primary ions. (Int J Mass Spectrom 207 (2001) 167–182) © 2001 Elsevier Science B.V.

Keywords: PTR-MS calibration; $H_3O^+ \cdot (H_2O)_n$ cluster ion distribution; Benzene and toluene; Humidity dependence

1. Introduction

Volatile organic compounds (VOCs) play a central role in the processes that generate tropospheric ozone and photochemical urban smog [1]. Especially in urban areas, aromatic hydrocarbons are of great interest not only because of their high ozone-forming potential (e.g., [2]) but also because of their health effects [3]. The sources for aromatic hydrocarbons in the atmosphere are mainly from anthropogenic origin. They constitute a substantial fraction of gasoline and also, therefore, of the nonmethane hydrocarbon (NMHC) emissions from traffic [4]. The main atmospheric removal pathway for aromatic hydrocarbons is the reaction with hydroxyl radicals (OH), and the corresponding atmospheric lifetimes vary from a few hours to many days [5]. As a result, they can be transported over large distances and play a role in the photochemistry of nonurban areas as well. After prolonged photochemical degradation of an air mass, the ratio between benzene and toluene concentrations is increased [6], which can be used as an indicator for the photochemical age of an air mass, that is, the time span between emission and sampling of pollutants [7].

The most common method for measuring benzene and toluene in ambient air is flask sampling and gas chromatographic (GC) analysis [8]. Only recently

*Corresponding author. E-mail c.warneke@phys.uu.nl

PII S1387-3806(01)00366-9

have other methods for measuring aromatics like DOAS (differential optical absorption spectrometry) [9] or CIMS (chemical ionization mass spectrometry) [10,11] been reported. In this work, we develop the use of proton-transfer-reaction mass spectrometry (PTR-MS) for on-line measurements of benzene and toluene in ambient air. PTR-MS is a recent technique that enables measurements of a wide variety of volatile organic compounds in ambient air with a high sensitivity and rapid time response [12]. In PTR-MS, chemical ionization of organic trace gases is achieved using proton-transfer reactions with H_3O^+ ions in a flow reactor. The product ions are extracted from the gas flow and mass analyzed with a quadrupole mass spectrometer. PTR-MS has been used successfully in atmospheric measurements from the ground, aircraft, and ships [13–15] and is also a useful tool in many laboratory applications [16–18].

When sampling humid air with PTR-MS, the H_3O^+ reagent ions become hydrated; that is, they form $H_3O^+ \cdot (H_2O)_n$ cluster ions. The presence of these ions would complicate the interpretation of the mass spectra; this problem is solved in PTR-MS by applying an electric field over the entire length of the flow reactor. This enhances the ion kinetic energy and reduces cluster formation. Usually the PTR-MS is operated at drift pressures of 1 mbar or less and an E/N of $\sim$140 Td (1 Td = 1 Townsend = 10^{-17} V cm^2). Under these conditions, the sum of the $H_3O^+ \cdot (H_2O)_n$ cluster fractions is kept $<$15% of the H_3O^+ ion signal [12] and typical ion count rates of 10–20 cps ppbv^{-1} (cps = ion counts per second; ppbv = parts per billion by volume) for any VOC in the air to be analyzed can be achieved. In order to obtain higher count rates and thus a higher sensitivity of the system, the reaction time (see Experimental section) needs to be enhanced, which is best done by increasing the drift pressure. We therefore operate the system at pressures of 2–3 mbar and obtain, as we will show later, count rates of 40–50 cps ppbv^{-1} of reactant VOCs. This, however, increases the fraction of $H_3O^+ \cdot (H_2O)_n$ cluster ions. For most of the compounds detectable with PTR-MS this is not a problem, since they react with both ions, and the product ions form less stable hydrates. For benzene and toluene, however, the reaction with $H_3O^+ \cdot (H_2O)$ is energetically not allowed and does not occur [19]. It is therefore expected, and is shown in this article, that the sensitivity of PTR-MS with respect to these compounds is reduced at a higher humidity of the sample air, that is, when the fraction of $H_3O^+ \cdot (H_2O)$ ions in the reactor is increased. The question then arises whether we can also understand the humidity effect quantitatively. In this article, a simple model is developed to calculate the distribution of $H_3O^+ \cdot (H_2O)_n$ cluster ions in the reactor. The model is validated by measuring the velocity of ions in the reactor, which gives some indirect information on the cluster ion distribution. The model is then used to explain the humidity dependence of the sensitivity toward benzene and toluene.

The influence of water vapor on the accuracy of SIFT-MS (selected ion flow mass spectrometry) measurements was studied earlier by Spanel and Smith [20]. The SIFT-MS uses proton transfer reactions involving H_3O^+ at thermal energy, and therefore, the measured cluster ion distribution is very sensitive to changes in humidity.

The method described here of measuring benzene and toluene in ambient air by PTR-MS was tested in the field by comparing PTR-MS results to GC analyses of gas samples. The humidity effect of the detection sensitivity could thus be verified. Also, since PTR-MS is a mass spectrometric technique, the possibility of interference from other compounds yielding product ions at the masses of benzene and toluene needs to be considered.

Finally, the implications of the present findings for the detection of other VOCs are investigated. The humidity dependence of the detection efficiency for isoprene is discussed in some detail because this compound does not react with higher $H_3O^+ \cdot (H_2O)_n$ ($n \geq 2$) cluster ions. Furthermore, the humidity effect is investigated for a number of other VOCs and the results are generalized and discussed.

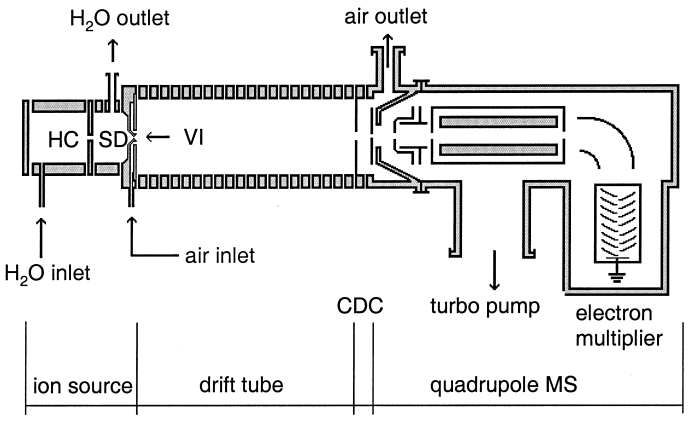

Fig. 1. A schematic representation of the PTR-MS. The ion source consists of a hollow cathode (HC) and a small drift region (SD), where all ions produced are converted into H_3O^+. Along the drift tube, an electric field is applied to provide a fixed *E*/*N*. The collisonal dissociation chamber (CDC) is used for fragmenting ions. In the detection system, the ions are mass filtered with a quadrupole mass spectrometer (MS) and counted with an electron multiplier.

2. Experimental

A detailed description of the PTR-MS technique can be found elsewhere [12]. A schematic drawing of the instrument is presented in Fig. 1. The PTR-MS consists of an ion source, a drift tube, where the ion molecule reactions take place and a quadrupole mass spectrometer. In a hollow cathode discharge (HC) ion source, H_3O^+ ions are produced from a pure water vapor flow of 8 STP cm^3 min^{-1} (STP: p = 1 atm and T = 273.15 K) in such a high purity that no mass filter is needed to preselect the hydronium ions. The ion source includes a small drift region (SD) where the ions produced in the HC have time to convert to H_3O^+. Through the Venturi inlet (VI), the reagent ions enter the drift tube, through which the sample air is pumped at a flow of ~30 STP cm^3 min^{-1}. Most of the water vapor in the ion source is removed by a turbo pump, but a small fraction of the water can enter the drift region via the Venturi inlet, leading to an extra moistening of the sample air in the drift tube.

In the drift tube, trace gases *R* in the sample air can be ionized by proton-transfer reactions with H_3O^+ ions:

$$H_3O^+ + R \rightarrow RH^+ + H_2O. \quad (1)$$

This reaction is exothermic and very efficient for those compounds *R* with a proton affinity higher than that of water. This includes many of the organic trace compounds present in the atmosphere, in which case the reaction proceeds at the collision rate of about 1 to 4×10^{-9} cm^3 $molecule^{-1}$ s^{-1}. Proton transfer does not occur for the more abundant trace compounds carbon dioxide, methane, nitrous oxide, carbon monoxide, and ozone. The count rate of RH^+ ions, $i(RH^+)$, can be calculated from

$$i(RH^+) = i(H_3O^+)_0\,(1 - e^{-k[R]t}) \approx i(H_3O^+)_0 k[R]t, \quad (2)$$

where $i(H_3O^+)$ is the count rate of H_3O^+ ions, *k* is the proton-transfer reaction rate coefficient, [*R*] the number density of trace molecules *R* in the reactor, and *t* the transit time of H_3O^+ ions. In this equation, it is assumed that the H_3O^+ and RH^+ ions are detected with the same efficiency. From the equation it can be seen that $i(RH^+)$ is proportional to [*R*], in other words, the signal is linear in the concentration of a trace gas. The sensitivity of PTR-MS with respect to a certain compound is measured and calculated in this article. It is defined as the number of product ions produced at a trace gas mixing ratio of 1 ppbv and at a H_3O^+ signal of 1 million ion counts per second (ncps $ppbv^{-1}$). The sensitivity is normalized to this typical number of reagent ions because the reagent ion signal can change both over time and slightly during a measurement.

The sensitivity is measured in this work using two calibrated standard mixtures. The first mixture contains benzene and toluene, among other compounds, in nitrogen at volume mixing ratios of 20 ppbv. The second mixture contains 1650 ppbv acetonitrile, 1020 ppbv acetaldehyde, 830 ppbv acetone, and 1210 ppbv isoprene in nitrogen. The two standards are further diluted with synthetic air using two calibrated flow controllers. Furthermore, the flow of synthetic air can be humidified using a commercial dew point generator (LI-COR LI 610, Lincoln, NE). Thus, a flow of air is obtained with a variable humidity and with VOCs at typical mixing ratios for both polluted and clean conditions. The VOC mixing ratio can also be varied to verify the linearity of the output signal. The accuracy of the standards should be better than 10%, as was stated by the producing company, but a comparison of different standards showed that an accuracy of only ~20% is obtained.

The sensitivity of PTR-MS with respect to a certain compound is calculated using Eq. (2). The rate coefficients for the proton-transfer reactions between H_3O^+ and benzene and toluene are given by $1.9 \pm 0.4 \times 10^{-9}$ cm^3 $molecule^{-1}$ s^{-1} and $2.2 \pm 0.4 \times 10^{-9}$ cm^3 $molecule^{-1}$ s^{-1}, respectively [21]. The reaction time can be calculated and measured. In this work we prefer to use the measured reaction time. In the calculation, the ion drift velocity v_d is estimated by $\mu \times E$, where μ is the ion mobility and E the electric field in the drift tube. The ion mobilities of the $H_3O^+ \cdot (H_2O)_n$ cluster ions in N_2 are given by Dotan et al. [22]. Measuring the reaction time is done by applying two short (10 μs) voltage pulses, first, to the orifice through which the ions are injected into the drift tube and, second, to the orifice through which the ions leave the drift tube and enter the collisional dissociation chamber (CDC). The voltage pulses cause a short disturbance in the otherwise constant signal of reagent ions. The arrival times of the disturbances at the detector are measured using a multichannel analyzer, which is triggered by the initial voltage pulse. The difference between the arrival times of the disturbances gives the reaction time t of ions in the drift tube. Furthermore, in the calculation of the sensitivity, the difference in detection efficiencies for the reagent and product ions is taken into account. The accuracy of the calculated sensitivity is mostly limited by the uncertainties in the values for k, which is ~20% for benzene and toluene [21].

A small amount of water from the ion source reaches the drift tube, leading to an extra moistening of the sample air. It is important to determine this amount because it means that, even when sampling dry air, the air in the drift tube contains water vapor and that cluster formation reactions of the H_3O^+ reagent ions with water molecules are possible:

$$H_3O^+ + (H_2O)_n(+M) \rightarrow H_3O^+ \cdot (H_2O)_n(+M). \quad (3)$$

We have estimated the flow of water vapor from the ion source to the drift tube by measuring the signal of $H_3O^+ \cdot (H_2O)$ ions as a function of the relative humidity of the sample air. At a certain pressure, electric field, and temperature, the $H_3O^+ \cdot (H_2O)$ ion signal is, in a good approximation, linearly dependent on the relative humidity. By extrapolating the measurements to the point where the $H_3O^+ \cdot (H_2O)$ ion signal is 0, the amount of water inside the drift tube was determined to be equivalent to ~45% relative humidity at 23°C of the sampled air. This corresponds to a flow of 0.4 STP cm^3 min^{-1} of water; that is, ~5% of the water flow in the ion source reaches the drift tube.

A small chamber is located between the drift tube and the detection system where the sample air is pumped away by a turbo pump. The chamber separates the high pressure in the drift tube (2.5 mbar) from the high vacuum (10^{-5} mbar) in the quadrupole chamber. This intermediate chamber also provides the possibility of performing collision-induced dissociation (CID) on the ions exiting the drift tube, and it is therefore called a collisional dissociation chamber (CDC) in Fig. 1. In typical conditions, the CDC is used such that cluster ions exiting the drift tube are fragmented into the core ions but not into smaller fragments. The advantage is that very few cluster ions are present in the mass spectra, which makes them easier to interpret and increases the signal intensity at the mass of the core ion. The disadvantage is that the

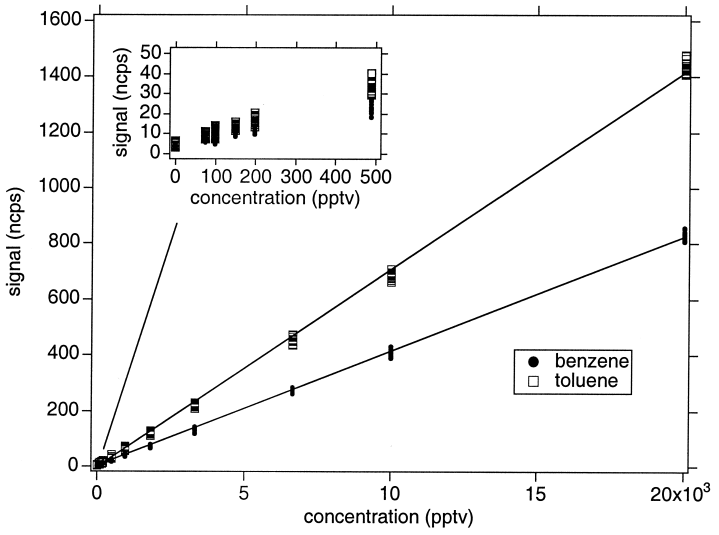

Fig. 2. Calibration curve of benzene and toluene in dry synthetic air for typical atmospheric concentrations.

mass spectra do not give an accurate representation of the ions present in the drift tube. This will be demonstrated further below, when the measured distribution of $H_3O^+ \cdot (H_2O)_n$ cluster ions is compared with a simple model calculation.

The air inlet of the PTR-MS system is made entirely from PFA Teflon to minimize memory effects on surfaces. For many volatile organic compounds, Teflon has proven to be the best material for inlet systems (e.g., [23]). The pressure in the drift tube has to be maintained at a constant value of typically 2.5 mbar, regardless of the ambient pressure. This is done using an off-line pressure controller (Bronkhorst, Veenendaal, Netherlands), which varies the airflow through the gas inlet to maintain a constant pressure of 200 mbar in the inlet. The further pressure drop from 200 mbar to the drift tube, operated between 1 and 3 mbar during this study, was generated using ~30 cm 1/16-in Teflon tubing. The setup guarantees a constant pressure in the drift tube and minimizes memory effects.

For intercomparison purposes, we also used gas chromatographic (GC) analyses of canister samples to measure benzene and toluene in ambient air. The GC is equipped with a flame ionization detector (FID) for NMHCs and an electron capture detector (ECD) for halocarbons. The sampling procedure and the GC system are described in detail by Lelieveld et al. [24]. The air samples were collected in 2.5-L electropolished stainless steel canisters. A metal bellows pump was used to flush the canisters ~5 min before filling them to 2.5 bar overpressure within 15 s. The canisters were transported to the laboratory and analyzed within a week. Before injection into the GC column, 500 cm^3 of the sample was preconcentrated in a liquid nitrogen cooled trap. The column used in the GC (Varian 3600, Walnut Creek, CA) is a capillary Silica Plot column (Chrompack, Middelburg, Netherlands) of 60 m × 0.53 mm, where a Helium flow of 9 cm^3 min^{-1} is used as a carrier gas. The detection limit of the GC measurements is a few pptv for hydrocarbons. Accuracy and precision of the GC measurements reported below were about ±20% for benzene and toluene.

3. Results and discussion

3.1. Humidity dependence of the sensitivity

A typical calibration curve for benzene and toluene in dry synthetic air is shown in Fig. 2. Protonated benzene is detected on mass 79 (amu) and toluene on mass 93 (amu). The conditions at which the system

was operated during this measurement were drift pressure 2.5 mbar and electric field 65 V cm^{-1}. The concentrations used in this measurement cover a range corresponding to values found in very polluted urban air (~20 ppbv) [25] to almost clean background air (<100 pptv [parts per trillion by volume]) [26]. The response of the instrument in ncps is linear in the covered range even at very low concentrations, which can be seen in the small panel in Fig. 2. These two masses are rather unique for these two compounds, and not much interference from other compounds is expected in gas analysis measurements.

The slope of a linear fit of the calibration curve defines the sensitivity, which is given in units of ncps $ppbv^{-1}$. The defined sensitivity assumes 1×10^6 cps H_3O^+ primary ions. In dry synthetic air, the sensitivity for benzene is 42 ncps $ppbv^{-1}$, and for toluene it is 71 ncps $ppbv^{-1}$. In this experiment, the number of H_3O^+ primary ions was $\sim 2.5 \times 10^6$ cps, so the actual ion count rates on mass 79 and mass 93 were a factor of 2.5 higher than the sensitivity (105 cps $ppbv^{-1}$ and 177 cps $ppbv^{-1}$, respectively). The measured sensitivity toward benzene is lower than toward toluene by a factor of 1.7 ± 0.5, where the uncertainty is because of the limited accuracy of the gas standard. The rate constants for the reaction of benzene and toluene with H_3O^+ are $1.9 \pm 0.4 \times 10^{-9}$ cm^3 $molecule^{-1}$ s^{-1} and $2.2 \pm 0.4 \times 10^{-9}$ cm^3 $molecule^{-1}$ s^{-1}, respectively, so from this we expect the ratio between the sensitivities to be 1.2 ± 0.3, that is, in agreement with the measured ratio.

Fig. 2 also shows the detection limit for benzene and toluene of the PTR-MS. The background signals are ~4 ncps beause of impurities in the synthetic air and the instrument. Assuming that the noise is the square root of the number of counts, the signal to noise ratio 1 is for count rates of 3.5 ncps; that is, the detection limit is ~80 pptv for benzene and 48 pptv for toluene for a 1-s integration time. Increasing the integration time to 1 min, the number of counts increases a factor of 60, and therefore, the detection limit would decrease accordingly to 9 and 5 pptv, respectively. Note here also that this detection limit is determined for 1×10^6 primary ions and that the detection limit decreases at higher signals. Other compounds have different background signals and, therefore, different detection limits as well.

As mentioned in the introduction, benzene and toluene do react through proton transfer with H_3O^+, but they do not react with $H_3O^+ \cdot (H_2O)$ [19]. The density of the $H_3O^+ \cdot (H_2O)$ cluster ions in the drift tube is dependent on the humidity of the sample air. Moreover, the signals observed with the MS are not necessarily representative for the density of these ions in the drift tube because of unknown CID in the CDC to form H_3O^+ from $H_3O^+ \cdot (H_2O)$. Therefore, we investigated the humidity dependence of the sensitivity. In Fig. 3, the same calibration curves for benzene and toluene as in Fig. 2 are shown, but for five different relative humidities. The temperature during this experiment was 23°C, as during all the presented laboratory measurements. With the temperature and the relative humidity, the water mixing ratio can be calculated, but we prefer to show the results, if possible, dependent on the relative humidity, because it is a more commonly used parameter. The sensitivity decreases at higher humidities from 39 ncps $ppbv^{-1}$ at 20% relative humidity to 17 ncps $ppbv^{-1}$ at 100% for benzene and from 62 ncps $ppbv^{-1}$ to 37 ncps $ppbv^{-1}$ for toluene. To explain this effect quantitatively, we make a detailed study of the cluster ion distribution in the following section.

3.2. Cluster ion distribution

In Fig. 4, measured and calculated cluster ion distributions for three different drift pressures of 3.6, 3.0, and 2.3 mbar are shown. The relative humidity of the sampled air and the electric field were fixed at 100%, and $E = 65$ V cm^{-1}. A higher drift pressure leads to a lower kinetic energy and, therefore, to larger clusters, as can be seen from Fig. 4.

The calculation of the cluster ion distribution was done according to Lau et al. [27], who measured the equilibrium constants, K, for the clustering reaction between H_3O^+ and water for different temperatures. The resulting van 't Hoff plots provided values for the entropy, ΔS^0, and enthalpy, ΔH^0 change, which can be used to calculate the free energy change, ΔG^0 at different ion temperatures T_{ion} using the equation

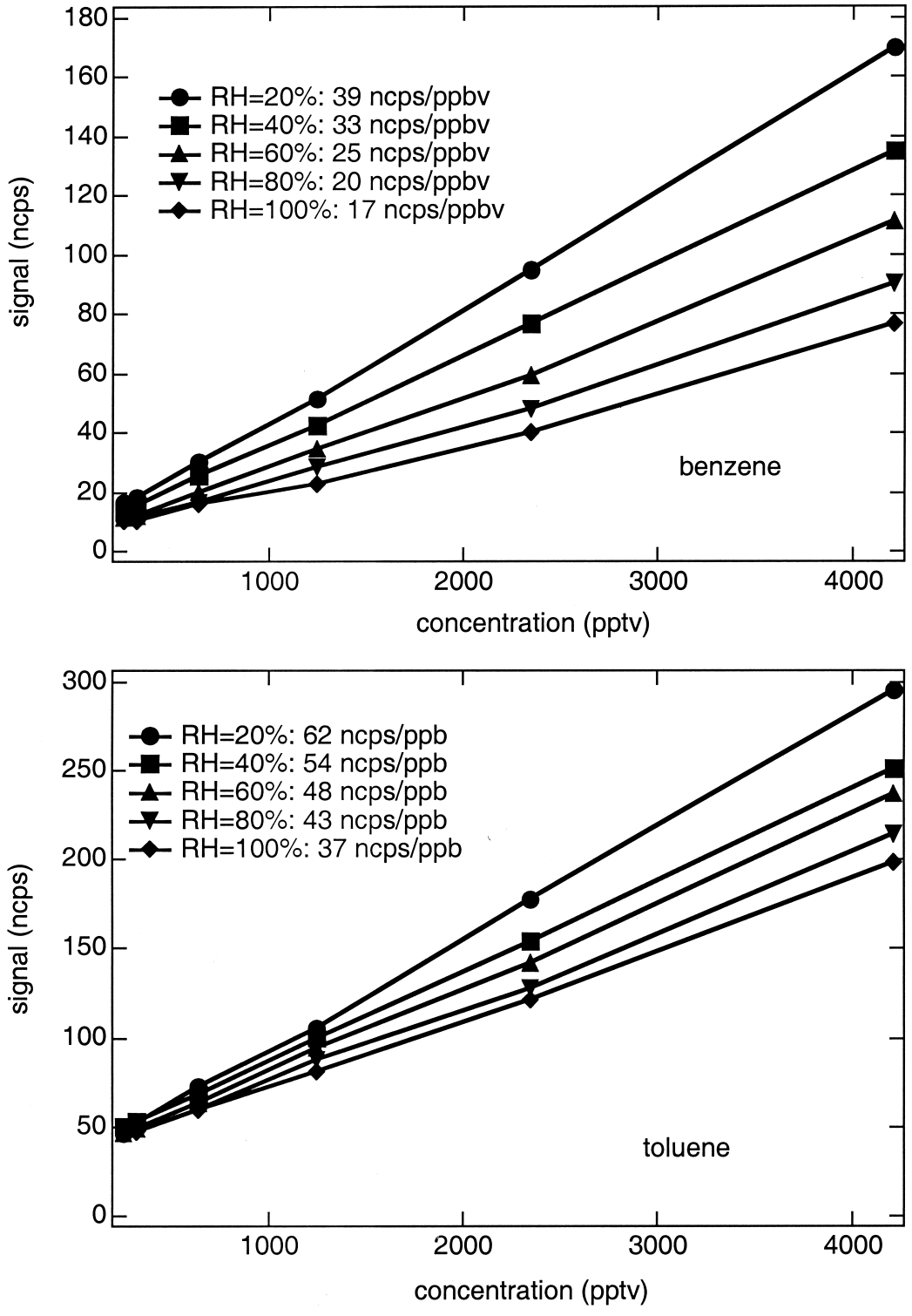

Fig. 3. Calibration curve of benzene and toluene in air using five different relative humidity values of the sampled air. (T = 23°C).

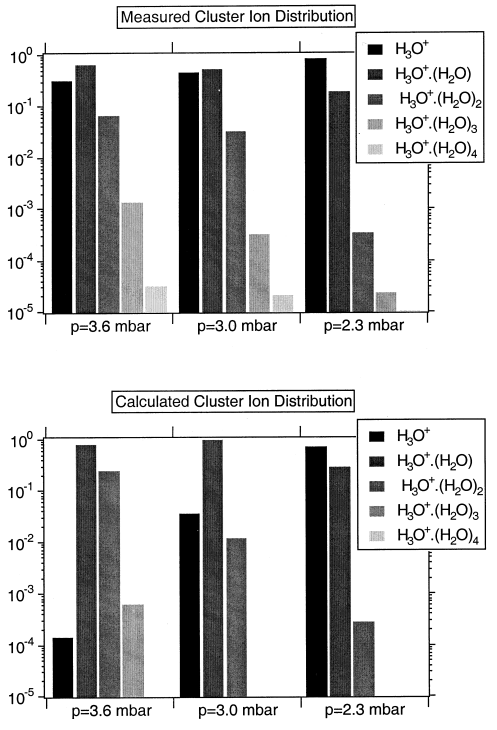

Fig. 4. The measured and calculated distribution of $H_3O^+ \cdot (H_2O)_n$ reagent ions at three different pressures ($E = 65$ V cm^{-1}; $RH = 100\%$, $T = 23$°C). The calculation of the cluster ion distribution was done according to Eqq. (4–6).

$$\Delta G^0 = \Delta H^0 - T_{ion}\Delta S^0 = -RT_{\text{ion}} \ln K. \quad (4)$$

We assume here that the ion temperature T_{ion} can be approximated by the effective temperature T_{eff} of the ions in the drift tube:

$$\frac{3}{2} kT_{\text{eff}} = \frac{3}{2} kT + \frac{1}{2} Mv_{\text{d}}^2. \quad (5)$$

The drift velocity v_{d} is given by

$$v_{\text{d}} = \mu E = \mu_0 \frac{p_0}{p} \frac{T}{T_0} E, \quad (6)$$

where μ_0 is the reduced mobility. The equilibrium constants in turn can be used to evaluate the relative concentrations of the hydrates $H_3O^+ \cdot (H_2O)_n$ for a wide range of gas pressures and effective temperatures, which is, in our case, equivalent to the electric field, and humidities.

In Fig. 4, it can be seen that the measured clusters are smaller than the modeled clusters. For example, looking at the H_3O^+ signal at 3.6 mbar, we measured ~30% of the primary ions, whereas the model shows a negligible amount for that signal. The reason for this might be the CID in the CDC, which our model calculation does not take into account. This leads to the conclusion that the measured H_3O^+ signal does not necessarily represent the H_3O^+ present in the drift tube. So the question arises of how many H_3O^+ ions are actually available in the drift tube to react with benzene and toluene.

3.3. Ion velocity measurements

The cluster ion distribution is strongly dependent on the velocity of the ions, as can be seen from Eqq. (4) and (5). A measurement of the velocity of the ions in the drift tube may help to describe the actual cluster ion distribution because this measurement concerns only the ions in the drift tube and no influence of the CDC is expected.

The reaction times of H_3O^+ and $H_3O^+ \cdot (H_2O)$ in air were measured and used to calculate the ion velocity and, from this, the mobility, μ, at different E/N values, using Eq. (6). The equation E/N is the characteristic parameter for the mobility, where N is the number density of the buffer gas molecules. In Fig. 5, the measured mobility of H_3O^+ (open symbols) and $H_3O^+ \cdot (H_2O)$ (full symbols) in air is plotted against E/N. For this experiment, three different relative humidities at 23°C were used. Also shown in the plot are measurements of the reduced mobilities of the same ions in N_2 taken from Dotan et al. [22], indicated in Fig. 5 with the dotted lines.

From Fig. 5, it can be seen that in the drift reactor of the PTR-MS, H_3O^+, and $H_3O^+ \cdot (H_2O)$ have the same reduced mobility at E/N values up to ~100 Td. At first sight this seems surprising, as the reduced mobilities of these ions traveling in nitrogen are different: The zero-field values are 2.76 cm^2 V^{-1} s^{-1} and 2.28 cm^2 V^{-1} s^{-1}, respectively. The difference between the measurements reported by Dotan et al. [22] and ours is the amount of water present in the buffer gas. In the PTR-MS drift tube, so many water molecules are present that the production of cluster

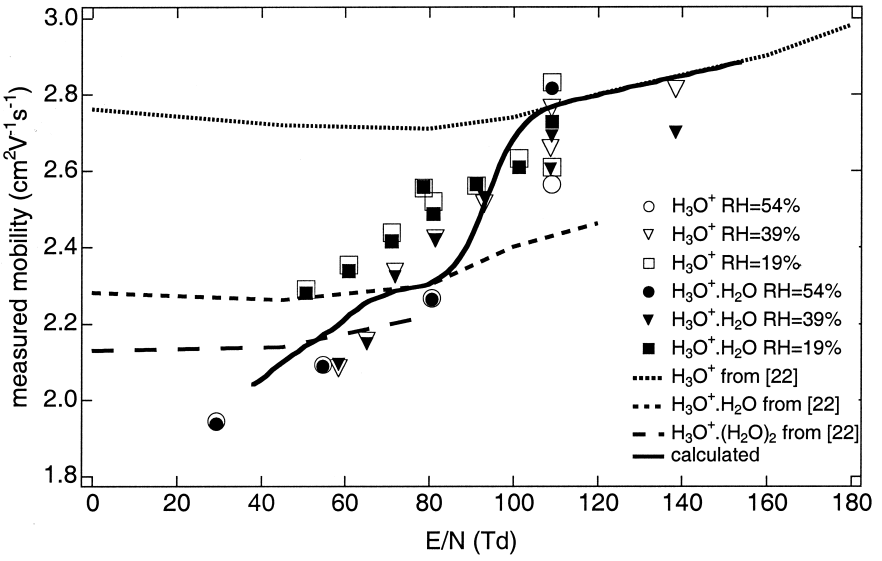

Fig. 5. Mobilities of H_3O^+ and $H_3O^+ \cdot (H_2O)$ measured in the PTR-MS at $T = 23$°C. The dotted lines show mobility measurements of the same ions and $H_3O^+ \cdot (H_2O)_2$ in nitrogen from Dotan et al. [22]. The solid curve was calculated using the values of Dotan et al. [22] weighted with the number density of respective cluster ions done according to Eqq. (4–6).

ions and the collision-induced dissociation are in equilibrium [27]. An individual ion in the drift region will undergo so many clustering reactions with neutral water and successive fragmentation that it spends part of its reaction time in its hydrated form and also in its unhydrated form. Therefore, the measured mobility will be the weighted average of the mobilities of the different cluster ions, where the weights are given by the respective number densities of H_3O^+ and $H_3O^+ \cdot (H_2O)_n$. This explains why at high *E*/*N*, the measured mobilities agree with the values obtained by Dotan et al. [22] for H_3O^+, whereas below 80 Td, the measurements agree better with the mobilities of $H_3O^+ \cdot (H_2O)$ and $H_3O^+ \cdot (H_2O)_2$. At an even lower *E*/*N*, the larger cluster ions gain more and more importance, which can be seen in the even lower measured mobility. At a higher *E*/*N* of ∼140 Td, a difference between H_3O^+ and $H_3O^+ \cdot (H_2O)$ can be seen.

Using this averaging procedure, the mobility of ions in the PTR-MS was calculated for a relative humidity of 55% of the sampled air. According to Eqq. (4), (5), and (6), the cluster ion distribution was calculated for different *E*/*N* values at the same relative humidity of the sampled air, taking the water from the ion source into account. The resulting relative number densities of $H_3O^+ \cdot (H_2O)_n$ ($n = 0, 1, 2$) were used to weigh the reduced mobility values taken from Dotan et al. [22]. For $H_3O^+ \cdot (H_2O)_3$, a zero-field reduced mobility of 2.0 $cm^2\ V^{-1}\ s^{-1}$ was assumed. The result of this averaging procedure is shown as a solid line in Fig. 2. The calculated mobility is in good agreement with the measured values. This suggests that the cluster ion distribution in the drift tube is as calculated from Eqq. (4), (5), and (6) and not as we measured with the MS. If we would use the measured cluster distribution as the weight for the averaging of the mobilities, we would get mobility values between the ones of H_3O^+ and $H_3O^+ \cdot (H_2O)$, which are much higher than the measurement shows.

3.4. Calculation of sensitivity versus humidity

The measurements of the reaction time and the cluster ion distribution provide a very good understanding of the processes inside the reaction chamber and the CDC. With this knowledge and the known ion chemistry of $H_3O^+ \cdot (H_2O)_n$ ($n = 0, 1, 2$), it is

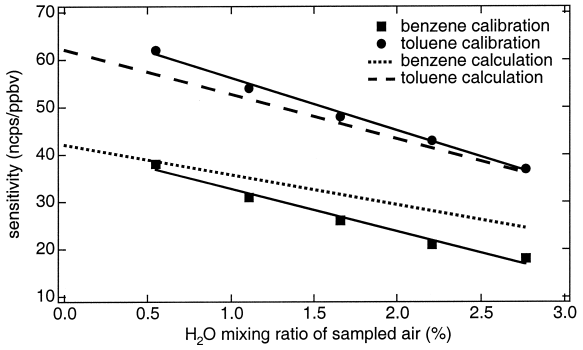

Fig. 6. The sensitivity for benzene and toluene as a function of the mixing ratio of water vapor in the sampled air. The measured values are from Fig. 3. The calculated curve is described in the text.

possible to calculate the humidity dependence of the sensitivity.

Using an H_3O^+ ion signal, which was corrected according to our model for humidity and fragmentation, the rate constants and the measured mobility of H_3O^+ in air, the sensitivity for benzene and toluene can be calculated for the humidities used in the experiment shown in Fig. 3. The result of this calculation is shown in Fig. 6 together with the measured sensitivities taken from Fig. 3. Here we plot the sensitivity against the water mixing ratio in the drift tube in order to make this result, which we want to use in further measurements, more general for every temperature and relative humidity. The calculation and the measurement are in good agreement with each other, especially as the cluster distribution, and hence the calculated sensitivity of benzene and toluene, is extremely sensitive to small changes in pressure and electric field. The slope of the calculated curve is characterized by system parameters influencing the cluster ion distribution. Here the agreement with the measurement is very good. The small difference in the absolute value might be because of the uncertainty in the rate constant and the concentrations in the standard mixture, as described earlier. This good agreement of the calculated sensitivity, where all instrument parameters have to be used, and the measured sensitivity, where a calibrated gas mixture was used, improves the confidence in our description of the processes going on in the PTR-MS instrument.

3.5. Intercomparison

In field measurements, where the conditions like temperature, pressure, or humidity change rapidly, it is important to conduct calibration measurements and not rely totally on the calculations. The changing conditions can influence not only the ion chemistry processes, as we have seen, but also the inlet system. This influence cannot be reasonably accounted for in any calculation. If possible, calibrations should be done by adding the calibration gas to the front of the inlet system to rule out background or memory effects in the system or tubing. Possible interference of other VOCs leading to ions with the same mass gives another reason for doing intercomparisons. Moreover, we want to verify the laboratory measurements, which were necessary for calculating the concentrations of VOCs in air, and to prove the capability of the PTR-MS instrument to measure benzene and toluene in ambient air correctly.

For an intercomparison measurement, the PTR-MS was deployed at Cabauw, the Netherlands, to measure on-line ambient air together with a system for sampling air in stainless steel canisters. Cabauw is a site $<$50 km away from some major Dutch cities in the center of the Netherlands. Continuous measurements of meteorological conditions and NO, NO_2, and ozone are made at this measurement site.

In Fig. 7, the time series of benzene and toluene are shown together with the result from GC analyses of nine sample canisters. In the small panel, a period of $\sim$12 h is enlarged, where five of the canisters were taken. The calculation of the concentration of the PTR-MS measurement was done using the measured sensitivity curve, as was shown in Fig. 6, dependent on the water vapor mixing ratio calculated from measured temperature and relative humidity, which lay between 60% and 100% and 5°–15°C during the measurement time. The temperature and the relative humidity are shown in the upper panel of Fig. 7. The calibration of the GC was done using the same calibrated gas mixture. The concentrations obtained with the two different instruments are in excellent agreement. In the small panel especially, the good agreement can be seen, where both instruments cover

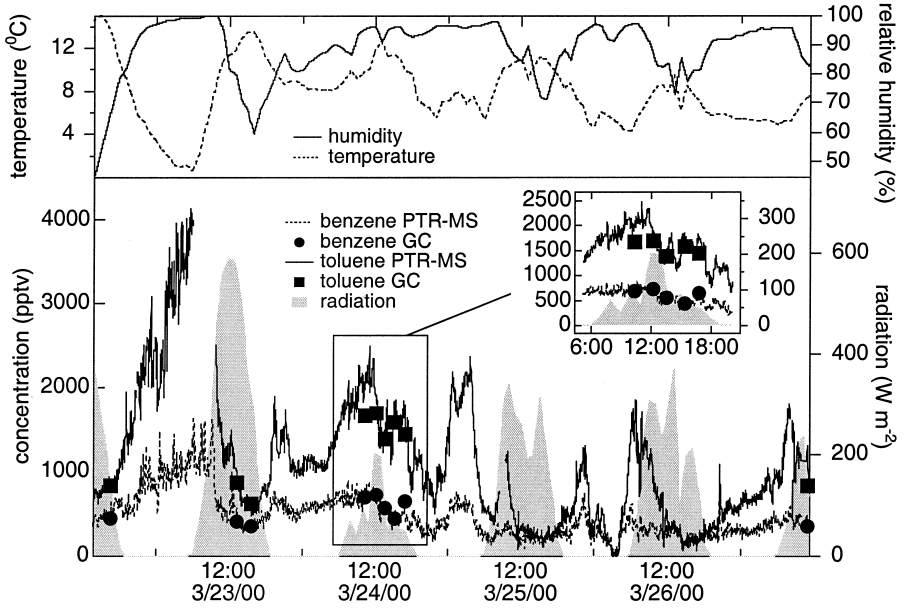

Fig. 7. Time series of benzene and toluene measured on-line with the PTR-MS and from canister samples with a GC-FID. The measurements were performed at Cabauw, The Netherlands, which is a quasi-urban site close to some major Dutch cities.

even small-scale variations in concentration. The correlation between the GC and PTR-MS results are shown in Fig. 8. The values for the PTR-MS measurements shown here are averages over the sample period of the respective canister. The slope of the linear fit from the correlation plot is close to 1: 0.82 ± 0.14 for benzene and 1.18 ± 0.11 toluene. This is just within the measurement precision for both instruments. The sampling of air in the stainless steel canisters can be responsible for this difference.

The average benzene concentration over the measurement period is 440 pptv and the concentration of toluene is 950 pptv. This gives a volume mixing ratio for benzene/toluene of 0.46, which is in the range of

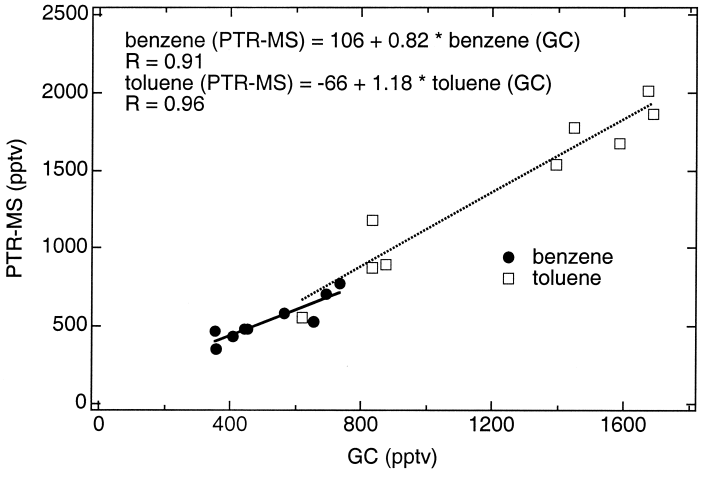

Fig. 8. Correlation between the GC and the PTR-MS measurements of benzene and toluene at Cabauw, The Netherlands.

the values given by Heeb et al. [11] of 0.41–0.83 and by Hewitt [28] of 0.51. These values are measured from vehicle emissions, where the air is not photochemically processed. In our case, the air is transported to the measurement site within a few hours. Chemical removal of toluene by OH is faster than that of benzene, yielding a shorter lifetime. Therefore, the volume mixing ratio benzene/toluene should increase with the age of the air mass, although a few hours since the emission took place is not enough time to considerably change the ratio. However, volume-mixing ratios for single peaks vary from 0.38 to 0.66, indicating that photochemistry is processing the air.

In Fig. 7 also, the radiation is shown, giving an indication of the night and day cycle and also of the cloud cover. On most of the days, an early morning and a late afternoon peak can be seen in the measurements of the aromatics corresponding to the traffic pattern, which was also seen in earlier measurements on other locations (e.g., [29]).

Mass 107, possibly C_2-benzenes (xylenes, benzaldehyde, and ethyl benzene) and mass 121, possibly C_3-benzenes (trimethyl benzenes, methyl ethyl benzenes, and propyl benzene) were also measured with the PTR-MS. These aromatic hydrocarbons have a lifetime in the atmosphere because of reactions with OH of only a few hours, and they play a major role in urban photochemical smog production. The source for these higher aromatics is also mainly motor vehicle emissions, as is the case for benzene and toluene. The correlations between toluene, mass 107, mass 121, and benzene are shown in Fig. 9. The concentrations of these higher aromatics were calculated using the rate constants, reaction time, and ion count rates as was described for benzene and toluene, but no humidity dependence was taken into account. For this plot, all points were used. In general, the correlations are very good, with *R* coefficients of 0.90, 0.88, and 0.88, respectively. The ratios of benzene/toluene, benzene/mass 107, and benzene/mass 121 are 0.27, 0.54, and 1.1, respectively, which is also in good agreement with engine exhaust measurements of the C_2- and C_3-benzenes [11,28]. All this gives a strong indication that mass 107 and mass 121 are indeed the C_2- and C_3-benzenes. Accurate measurement of these compounds seems to be very important because there is evidence that previous assessments of reactive carbon species may have underestimated the contribution of higher aromatic compounds to the total VOCs leading to a larger pool of ozone forming carbon compounds [30].

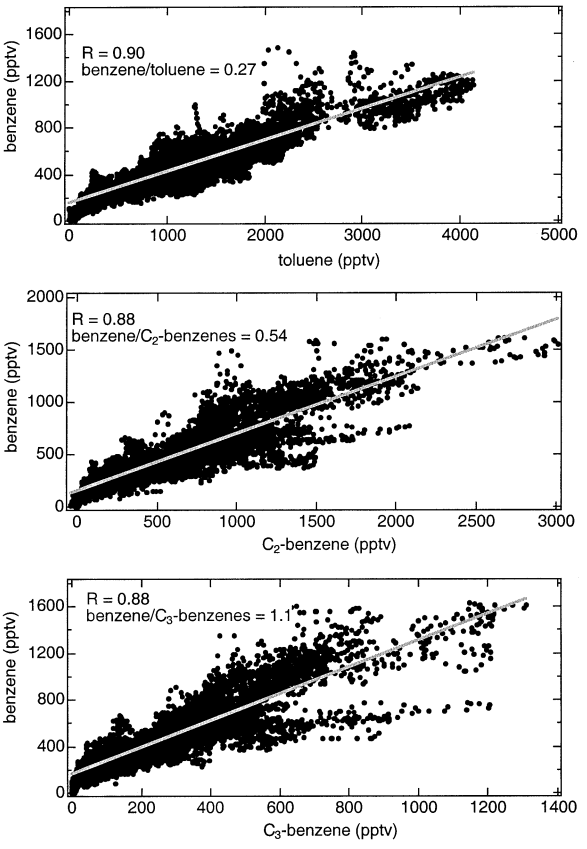

Fig. 9. Correlation between benzene, toluene, C_2-benzenes, and C_3-benzenes at Cabauw, The Netherlands. All data points from Fig. 7 are used in this figure.

3.6. Other compounds

Unlike benzene and toluene, most VOCs do react with $H_3O^+ \cdot (H_2O)_n$ cluster ions by proton transfer reactions,

$$H_3O^+ \cdot (H_2O)_n + R \rightarrow R \cdot H^+ + (n+1)H_2O, \quad (7)$$

and switching reactions,

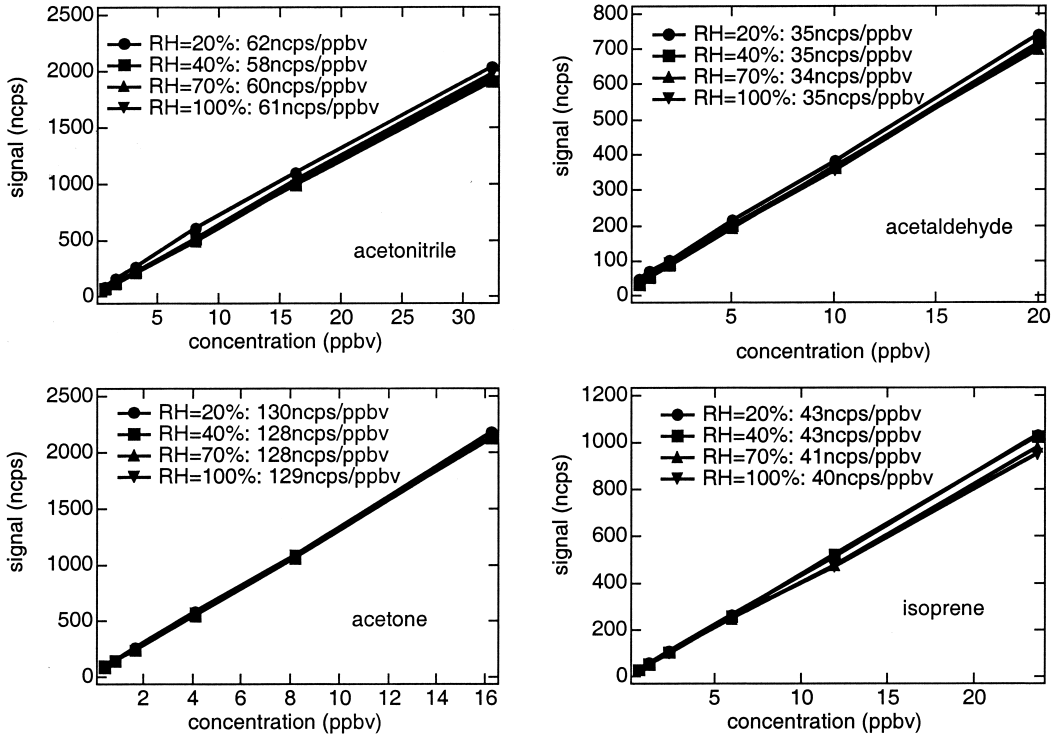

Fig. 10. Calibration measurements of acetonitrile, acetaldehyde, acetone, and isoprene at different relative humidities using a standard gas mixture (p = 2.5 mbar; E = 65 V cm^{-1}, T = 23°C).

$$H_3O^+ \cdot (H_2O)_n + R \rightarrow R \cdot H_3O^+ + nH_2O, \qquad (8)$$

Reaction (7) is allowed if the proton affinity of R is high enough, which is not the case for benzene and toluene. Their proton affinities (181.3 and 189.8 kcal mol^{-1}, respectively) [31] are too low. Reaction (8) seems to take place only if R has a certain dipole moment [19], which is not the case for benzene and toluene [32]. The product ion distributions and rate constants measured in a SIFT (selected ion-flow tube) for benzene and toluene and other VOCs for the reactions (7) and (8) can be found in Spanel and Smith [19]. The ratio between reactions (1), (7), and (8) cannot be measured in our system: The electric field in the CDC was chosen so high that cluster ions mainly break into their core ions. The result of the switching and subsequent fragmentation can be called dissociative switching reaction.

The effect of humidity on the sensitivity is not expected to be significant for compounds other than benzene and toluene because only a few nonpolar molecules with a higher proton affinity than water exist. Calibration curves at different humidities were measured for many different compounds. In Fig. 10, measurements for acetone (CH_3COCH_3), acetonitrile (CH_3CN), isoprene (C_5H_8), and acetaldehyde (CH_3CHO) are shown using another calibrated gas standard. The conditions in the drift tube were the same as in Fig. 3, with 2.5 mbar and 65 V cm^{-1}. No significant dependence on the humidity can be seen for these compounds. In Fig. 5, we have seen that so many reactions between H_3O^+ and $H_3O^+ \cdot (H_2O)_n$ take place that all these ions have the same velocity in the drift tube, leading to an average mobility even at lower relative humidity. The same accounts for the rate constant for the proton transfer and the dissociative switching reactions. The RH^+ ions are produced with an average rate constant, and all hydrated hydronium ions act as primary ions, just like H_3O^+.

In a recent study, Spanel and Smith [20] have observed a humidity dependence of some polar compounds using H_3O^+ as primary ions in a SIFT-MS instrument. In a SIFT-MS, no electric field is applied to the drift tube and, therefore, it is operated at thermal energies. At this low kinetic energy, the cluster ion distribution is more sensitive to changes in humidity than is the PTR-MS. In the SIFT-MS, the predominant ions at high humidities are $H_3O^+ \cdot (H_2O)_3$, and because of the even small differences in values of k for proton transfer from H_3O^+ and for ligand switching with $H_3O^+ \cdot (H_2O)_3$, a humidity dependence was found. In the PTR-MS, the applied electric field prevents such a significant change in the cluster ion distribution, and no humidity dependence on polar compounds such as acetone was found in the work presented here.

One of the compounds measured in Fig. 10 is isoprene. Isoprene has a rather high proton affinity (200.4 kcal mol^{-1}) [31], so it can undergo proton transfer reactions with $H_3O^+ \cdot H_2O$ ions, but a small dipole moment (0.25 D) [32], and it does not react with larger cluster ions [19]. At low E/N, larger clusters may contribute significantly to the primary ions, and an effect on the sensitivity of the PTR-MS for isoprene can be expected. Using a higher drift pressure of 3 mbar yielding an E/N of 80 Td, the calibration of isoprene was repeated. In Fig. 11(a), the calibration curves for different relative humidities are shown. In contrast to the measurement with 2.5 mbar, a dependence of the sensitivity on the humidity can be noticed. The measured and calculated sensitivity is plotted against the relative humidity illustrated in Fig. 11(b). The sensitivity was calculated using an average rate constant of H_3O^+ and $H_3O^+ \cdot H_2O$ with isoprene of 1.9×10^{-9} cm^3 s^{-1} $molecule^{-1}$. The number of primary ions was calculated by adding the H_3O^+ and $H_3O^+ \cdot H_2O$ densities, which were determined using the cluster ion distribution calculation as earlier described. At a relative humidity of 100%, almost 30% of the primary ions are $H_3O^+ \cdot (H_2O)_2$; at 0% humidity, this number is only 5% according to the calculation. The agreement between the calibration and the calculation is still very good, especially looking at the slope, but not as good as for benzene and toluene because the calculation of the cluster ion distribution is expected to be more accurate for smaller cluster sizes. It seems as if the actual rate constant was taken a little bit too high. When measuring isoprene, it is important to use mainly H_3O^+ and $H_3O^+ \cdot H_2O$ reagent ions; otherwise, the sensitivity for isoprene would get too low.

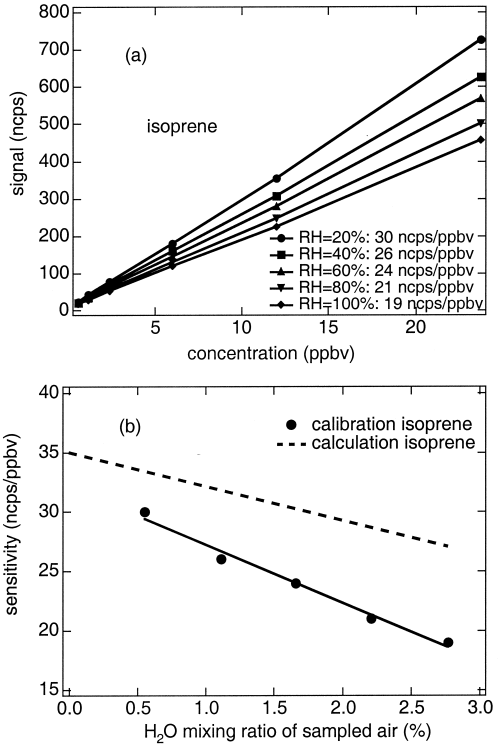

Fig. 11. (a) Calibration measurements of isoprene at different humidities at a higher drift pressure ($p = 3.0$ mbar; $E = 65$ V cm^{-1}, $T = 23$°C). (b) Calculated and measured sensitivity for isoprene versus the mixing ratio of water vapor in the sampled air. The calculation is described in the text.

The dependence on the relative humidity for other compounds such as dimethyl sulfide (DMS) (CH_3SCH_3), methanol (CH_3OH), acetic acid (CH_3COOH), and formaldehyde (CH_2O) was also investigated. The calibration curves of these compounds show no dependence on the humidity except for formaldehyde. The explanation is that formaldehyde has a proton affinity close to water with 171.7 kcal mol^{-1} [31]. The exothermicity of this reaction is therefore only 5.2 kcal mol^{-1}. Protonated formalde-

hyde can undergo a back reaction with the very abundant water molecules in the drift tube. The rate constant for this back reaction at the used center of mass energy (KE_{cm}) of 0.13 eV between H_3O^+ and formaldehyde is $\sim 2 \times 10^{-11}$ cm^3 s^{-1} [33]. At higher humidity, the back reaction is more efficient and, thus, the sensitivity for formaldehyde is decreased.

4. Conclusions

The work presented here demonstrates the ability of the PTR-MS to perform on-line measurements of aromatic compounds with a detection limit of <50 pptv and a time resolution of a few seconds. Laboratory experiments and field measurements were conducted to characterize the precision, sensitivity, and detection limit of the PTR-MS system.

Calibrations for benzene and toluene as well as other VOCs were performed at different relative humidities of the sample air. They agree very well with calculated values when taking the cluster ion distribution as a function of the humidity into account. In general, a humidity effect on the sensitivity can be expected for two classes of compounds. These are substances, such as benzene and toluene, that do not react with the hydrated hydronium ions and substances with a proton affinity close to water, such as formaldehyde. We have developed a simple model that calculates the cluster ion distribution in the drift tube. This model was verified by measuring the ion drift velocities. Using the model, it was possible to explain the dependence of the sensitivity on the humidity.

In a field experiment, the calibrated PTR-MS on-line measurements of benzene and toluene were intercompared with GC-FID analysis of canister samples. The agreement with the well-established GC technique was excellent. The experiment was conducted in a rather polluted area. We did not see an interference of benzene and toluene with other VOCs, so we do not expect an interference elsewhere either.

Further developments include improving the sensitivity and the selectivity of the PTR-MS. At a higher drift pressure, the sensitivity is increased, but the E/N should be kept constant. Otherwise, no unhydrated ions would be present, and the ability to measure benzene, toluene, and also isoprene would be lost. This cleary illustrates the importance of an electrical field applied to the drift tube. In atmospheric pressure CIMS instruments, where $H_3O^+ \cdot (H_2O)_n$ ions are used as reagent, these compounds are not expected to be detectable with the necessary sensitivity. Another way of increasing the sensitivity would be to increase the length of the drift tube and, therefore, the reaction time, but the loss of ions would increase as well, as a result of diffusion and collisions with the wall. Other than this, optimizing the ion source could increase the ion signal and, thus, the sensitivity. The selectivity could be improved by using different primary ions with different proton affinities to selectively ionize compounds with the same mass. This might help to identify the different higher aromatic compounds, which have the same mass. In this work, only the sum of the C_2- and C_3-benzenes could be measured, not the individual compounds. The identification of the different aromatics would help in air-quality measurements because they have different lifetimes and chemical pathways.

Acknowledgements

This work is part of the research program of the Foundation of Fundamental Research on Matter (FOM). We thank the KNMI (Royal Netherlands Meteorological Institute) for providing the humidity and radiation data and Michel Bolder and Bert Scheeren for preparing the canister sample system. We also want to thank Arend Niehaus and Jos Lelieveld for their support.

References

[1] S. Houweling, F. Dentener, J. Lelieveld, J. Geophys. Res. 103 (1998) 10673–10696.
[2] R.G. Derwent, M.E. Jenkin, S.M. Saunders, Atmos. Environ. 30 (1996) 181–199.
[3] WHO, Air Quality Guidelines for Europe, Geneva, CH. European Series 23, 1987.

[4] H.B. Singh, L.J. Salas, B.K. Cantrell, R.M. Redmont, Atmos. Environ. 19 (1985) 1911–1919.
[5] R. Atkinson, Atmos. Environ. 34 (2000) 2063–2101.
[6] R. Atkinson, Atmos. Environ. 24A (1990) 1–42.
[7] T.S. Clarksen, R.J. Martin, J. Rudolph, B.W.L. Graham, Atmos. Environ. 30 (1996) 569–577.
[8] D.D. Parrish, F.C. Fehsenfeld, Atmos. Environ. 34 (2000) 1921–1957.
[9] H. Edner, P. Ragnarson, S. Spaennare, S. Svanberg, Appl. Optics 32 (1993) 327–333.
[10] A. Hansel, A. Jordan, R. Holzinger, P. Prazeller, W. Vogel, W. Lindinger, Int. Mass Spectrom. Ion Processes 149/150 (1995) 609–619.
[11] N.V. Heeb, A.M. Forss, C. Bach, S. Reimann, A. Herzog, H.W. Jaeckle, Atmos. Environ. 34 (2000) 3103–3116.
[12] W. Lindinger, A. Hansel, A. Jordan, Int. J. Mass Spectrom. Ion Processes 173 (1998) 191–241.
[13] J. Williams, U. Pöschl, P.J. Crutzen, A. Hansel, R. Holzinger, C. Warneke, W. Lindinger, J. Lelieveld, J. Atmos. Chem. 38 (2001) 133–166.
[14] U. Pöschl, J. Williams, P. Hoor, H. Fischer, P.J. Crutzen, C. Warneke, R. Holzinger, A. Hansel, A. Jordan, W. Lindinger, H.A. Scheeren, J. Lelieveld, J. Atmos. Chem. 38 (2001), 115–132.
[15] C. Warneke, R. Holzinger, A. Hansel, W. Lindinger, J. Williams, U. Pöschl, P. Crutzen, J. Atmos. Chem. 38 (2001) 167–185.
[16] C. Warneke, T. Karl, H. Judmaier, A. Hansel, A. Jordan, W. Lindinger, P.J. Crutzen, Global Biogeochem. Cycles 13 (1999) 9–18.
[17] R. Holzinger, C. Warneke, A. Hansel, A. Jordan, W. Lindinger, D. Scharffe, G. Schade, P.J. Crutzen, Geophys. Res. Lett. 26 (1999) 1161–1164.
[18] J.A. de Gouw, C.J. Howard, T.J. Custer, R.Fall, Geophys. Res. Lett. 26 (1999) 811–814.
[19] P. Spanel, D. Smith, J. Phys. Chem. 99 (1995) 15551–15556.
[20] P. Spanel, D. Smith, Rapid Comm. Mass Spectrom. 14 (2000) 1898–1906.
[21] P. Spanel, D. Smith, Int. J. Mass Spectrom. Ion Processes 181 (1999) 1–10.
[22] I. Dotan, D.L. Albritton, W. Lindinger, M. Pahl, 11 65 (1976) 5028–5030.
[23] J.A. Neuman, L.G. Huey, T.B. Ryerson, D.W. Fahey, Environ. Sci. Technol. 33, (1999) 1133–1136.
[24] J. Lelieveld, A. Bregman, H.A. Scheeren, J. Ström, K.S. Carslaw, H. Fischer, P.C. Siegmund, F. Arnold, J. Geophys. Res. 104 (1999) 8201–8213.
[25] K. Kourtidis, I. Ziomas, C. Zerefos, A. Gousopoulos, D. Balis, P. Tzoumaka, Atmos. Environ. 34 (2000) 1471–1480.
[26] P.D. Goldan, W.C. Kuster, F. Fehsenfeld, S.A. Montzka, J. Geophys. Res. D12 100 (1995) 25945–25963.
[27] Y.K. Lau, S. Ikuta, P. Kebarle, J. Am. Chem. Soc. 104 (1982) 1462–1468.
[28] C.N. Hewitt, Reactive Hydrocarbons in the Atmosphere, London: Academic Press, 1999, chapter 1, p. 10.
[29] D. Brocco, R. Fratarcangeli, L. Lepore, M. Petricca, I. Ventrone, Atmos. Environ. 4 31 (1997) 557–566.
[30] A.C. Lewis, N. Carslaw, P.J. Marriott, R.M. Kinghorn, P. Morrison, A.L. Lee, K.D. Bartle, M.J. Pilling, Nature 405 (2000) 778–781.
[31] S.G. Lias, J.E. Bartmess, J.F. Liebman, J.L. Holmes, R.D. Levin, W.G. Mallard, J. Phys. Ref. Data (1988) 17(Suppl. 1).
[32] R.D. Nelson Jr., D.R. Lide Jr., A.A. Maryott, CRC Handbook of Chemistry. Cleveland, OH: CRC Press (1991).
[33] A. Hansel, W. Singer, A. Wisthaler, M. Schwarzmann, W. Lindinger, Int. J. Mass Spectrom. Ion Processes 167/168 (1997) 697–703.